Ten Years of Lake Taupō Surface Height Estimates Using the GNSS Interferometric Reflectometry

Lucas D. Holden

RMIT University, Melbourne, Australia

Kristine M. Larson

University of Colorado, Boulder, USA

Abstract

A continuously operating GNSS station within a lake interior is uncommon, but advantagous for testing the GNSS Inteferometric Reflectometry (GNSS-IR) technique. In this research, GNSS-IR is used to estimate ten years of lake surface heights for Lake Taupō in New Zealand. This is achieved using data collected from station TGHO, approximately 4 km from the lake's shoreline. Its reliability is assessed by comparisons with shoreline gauges and satellite radar altimetry lake surface heights. Relative RMS differences between the daily averaged lake gauge and GNSS-IR lake surface heights range from ±0.027 to ±0.028m. Relative RMS differences between the satellite radar altimetry lake surface heights and the GNSS-IR lake surface heights are ±0.069m and ±0.124m. The results show that the GNSS-IR technique at Lake Taupō can provide reliable lake surface height estimates in a terrestrial reference frame. A new ground-based absolute satellite radar altimetry calibration/validation approach based on GNSS-IR is proposed and discussed.

Keywords

GNSS, Reflectometry, Satellite Radar Altimetry, Lake Surface Height

Introduction

Since GNSS reflectometry was originally proposed by Martin-Neira (1993), a variety of experiments have been conducted using reflected GNSS signals to measure water levels. Initially, equipment was designed or altered in some way to enhance the reflections (Anderson 2000; Treuhaft et al. 2001; Dunne et al. 2005; Löfgren et al. 2009). More recently, standard pointing geodetic-quality GNSS instruments, that are nominally designed to suppress GNSS reflections, have been used (Larson et al. 2013a; Roussel et al. 2015; Santamaria-Gomez et al. 2015; Strandberg et al. 2016). This method is often called GNSS Interferometric Reflectometry (GNSS-IR) because it is based on the interference pattern created by the direct and reflected signals from a single instrument. The advantage of using a GNSS receiver to achieve this is that it can simultaneously measure three-dimensional position (using the carrier phase data) and water surface levels (using the engineering signal strength data), placing the measurements in a well-defined terrestrial reference frame. This accommodates regional or local deformation processes. While some lake gauges worldwide are well defined in a terrestrial reference frame, many are not.

There have been many comparisons between GNSS-IR and tide gauges, however only one has looked at long-term stability over a decade (Larson et al. 2017). Fewer GNSS-IR studies have focussed on continental water bodies. Song et al. (2019) showed an 8-month water level record from Shuandwangcheng Reservoir in China and reported an RMS error of 0.05m. Their truth values were measured by hand once per day. Sun (2017) used a 12-year GNSS-IR study of data from Lake Huron, but the emphasis was on lake ice and not continuous water level monitoring. Long-term comparisons remain essential to test the robustness of the GNSS-IR model across varying conditions.

The main contribution of this study is to examine the stability of GNSS-IR from 2009-2019 at Lake Taupō, New Zealand. We compare its performance with two traditional water gauges on the lakeshore (~15-20km away) and with community-developed satellite radar altimetry products. This comparison

is complicated by the presence of significant ground deformation at the shoreline gauges, but this itself is an important issue which we will highlight. Furthermore, the altimetry crossovers are not co-located with the GNSS site, which will be present in any altimetry product. Nevertheless, this is an opportunity to assess the different lake surface height measurement techniques, describe their limitations, and summarize how well they agree over a decade. The second significant contribution of this study is to propose a new ground-based satellite radar altimetry calibration/validation technique based on the GNSS-IR technique.

Basic Principles of GNSS Interferometry Reflectometry

The GNSS-IR fundamentals related to the measurement of water level are discussed by Larson et al. (2013a) and Roussel et al. (2015). The interference pattern is created by beating of the direct GNSS signal (used for positioning) and reflected GNSS signal (from below the antenna) (Fig. 1). The interference pattern is observed using Signal to Noise Ratio (SNR) or signal power data. The primary GNSS-IR observable equation for SNR data is:

$$SNR = A(e)\sin\left(2\pi \cdot \frac{2H_R}{\lambda}\sin e + \theta\right) \quad (1)$$

where H_R is the vertical distance between the antenna and the reflecting surface, (λ) is the GNSS transmitting wavelength, and e is the satellite elevation angle, which is defined with respect to the horizon. The phase offset θ is not used in water level retrievals. The amplitude (A) of the interference pattern is controlled by the type of surface (ice, soil, water) and its roughness. A also depends on e because a geodetic-quality GNSS antenna has been designed to enhance higher elevation angle tracking. The frequency of the SNR interference pattern is controlled by the geometry of the reflected signal (e, λ, and H_R). As H_R decreases, water level increases and vice versa. Since e and λ are known, H_R can be

estimated using straight-forward periodogram techniques. Because the data are unevenly sampled, the frequency is often estimated using a Lomb Scargle Periodogram as in Larson et al. (2013a).

In principle, H_R can be estimated for every rising and setting GNSS satellite arc. Each H_R value corresponds to the time-period of the rising or setting GNSS arc, ~30 minutes. For water level applications, azimuth and elevation angle masks must be set to ensure that the GNSS-IR signal reflects off the water. At GNSS sites where water levels are rapidly changing from tidal influences during a rising/setting arc, additional corrections are required (Larson et al. 2013b). Because Lake Taupō is a lake surface, this so-called $\dot{H}$ correction is not needed. Here a daily average of the individual arc H_R values can be used.

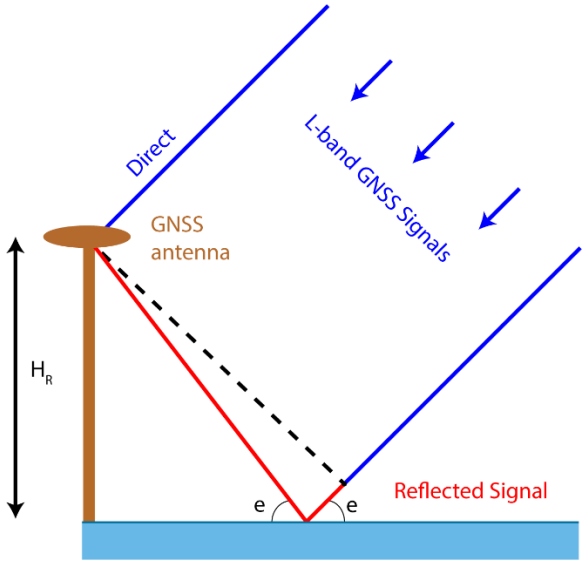

Fig. 1 Representation of reflected GNSS signal geometry**.** H_R is the vertical distance between the phase center of the GNSS antenna and the reflecting surface. e is the angle between the satellite and the horizon. The direct GNSS signals are shown in blue; the additional path travelled by the reflected signal is shown in red

Unfortunately, it is impossible to find a single precision value for H_R from the available GNSS-IR literature. The variation in results stems from multiple factors. First, every GNSS study has site-specific error sources related to multiple reflection surfaces at busy harbors, highly variable elevation and azimuth masks, and sites being relatively far from the water. Secondly, unlike GNSS carrier phase data, the quality of GNSS SNR data is more highly variable, with newer receivers generally reporting better quality high-rate data (multi-GNSS and GPS L2C, L5 signal) than the older receivers tracking only legacy GPS signals at low sample rate`s (30 sec). And finally, investigators have used different models in analysis of the SNR data. These models impose smoothness on temporal variations in water levels in a variety of ways that certainly improves precision, but generally makes it difficult to compare results.

Experiment Location and Data

TGHO is located on an anchored platform on the Horomatangi East Reef, approximately 4 km offshore on Lake Taupō, New Zealand (Fig. 2a). Lake Taupō has an approximate length and width of 46 and 33 km**,** respectively, a surface area of 660 km^2 and maximum depth of 186m. The lake level has been artificially controlled since 1941 (Eser and Rosen 2000). The lake surface height is measured hourly by gauges at Acacia Bay and Tokaanu, located at the north and south end of the lake**,** respectively (Fig. 2a). Wind direction and speed data are available from Lake Taupō airport (TAUP on Fig. 2a). Observations from TGHO, the two lake gauges, and the weather station were obtained for the period between January 2009 to the end of October 2019.

TGHO is part of the New Zealand national GNSS network to support crustal deformation research. Since installation it has been equipped with a Zephyr 2 antenna (2008 to present) and a Trimble NETRS (2008-2016) and NETR9 receiver (2016 to present). Except for a 232-day loss of data in 2017-2018, 94% of daily GPS data files were available. The TGHO data are provided with 30-second sampling. This particular receiver type is known to have fairly imprecise L1 C/A based SNR data (Larson and

Nievinski 2013). The L2P SNR data are degraded by the internal tracking algorithm used (Roesler and Larson 2018). The receiver tracks no modern GPS signals such as L2C and L5. Here we will use only the L1 signals and will not impose smoothing constraints (Strandberg et al. 2016; Reinking et al. 2019). We expect the individual water level retrievals to be less precise than studies with newer receivers, modern signals and those imposing smoothing constraints, but since we will focus on daily averages, we believe this will be adequate (Larson et al. 2017).

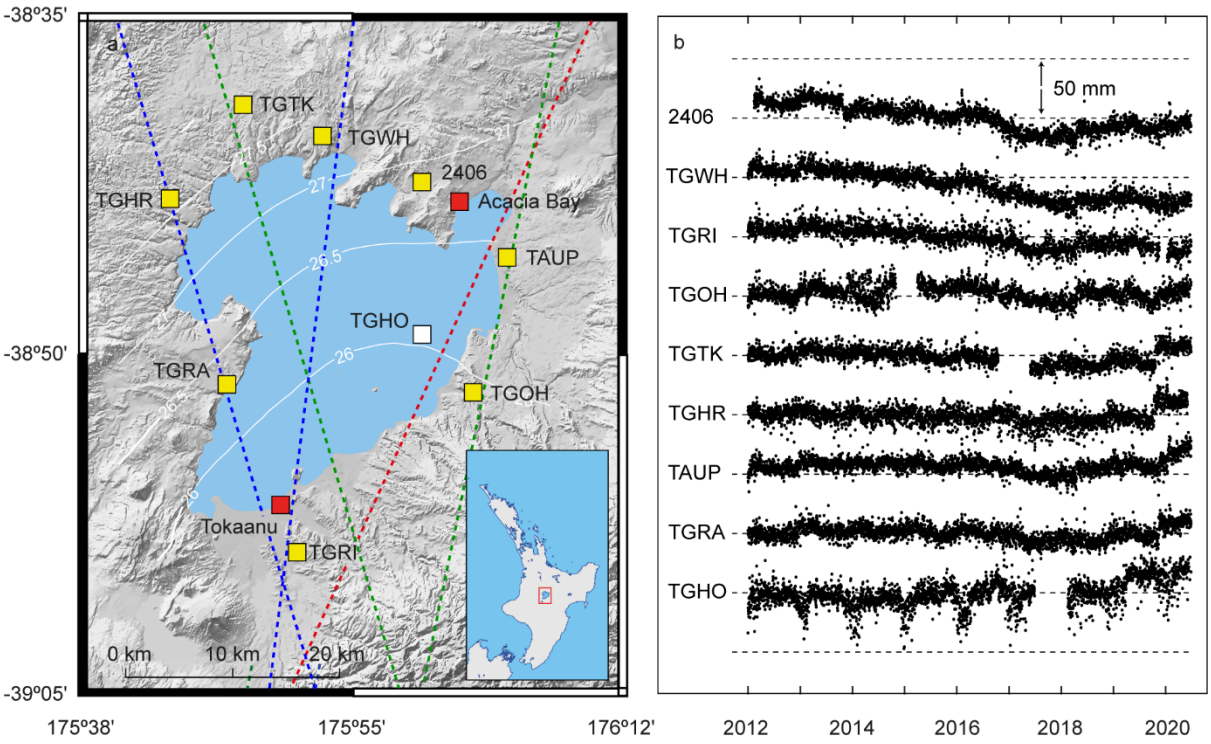

Fig. 2 a Location map. GNSS station TGHO is shown in white. The Acacia Bay and Tokaanu lake level gauges are shown in red. The location of nearby GNSS CORS stations are shown in yellow. The inset shows the location of Lake Taupō on the North Island. The white lines show the geoid-ellipsoid separation contours (m) for the region from NZGeoid2016. The dashed lines show the approximate ground track of the Jason-2 and 3 (red), Envisat/Saral (blue) and Sentinel 3a (green) satellite altimetry data used in the community-based G-REALM Lake Taupō and DAHITI products; **b** Change in ellipsoidal height time series (black dots) (ITRF2008 frame) for the GNSS CORS stations shown in Fig. 1a. The vertical spacing between the horizontal lines is 0.050m

TGHO is fixed on a platform above the lake surface, with a solar panel on the southside of the antenna (Fig. 3a). The antenna is fixed 0.750m above a platform suspended on three pillars anchored to Horomatangi reef (approximately 3.91 m above the water surface). There is a clear field of view over the lake surface from approximately WSW to ESE direction. A solar panel south of the antenna may block some signals from a southerly azimuth. Fortunately, few GNSS satellites pass through the southern sector of the sky at this station. This special environment is highly suitable for GNSS-IR.

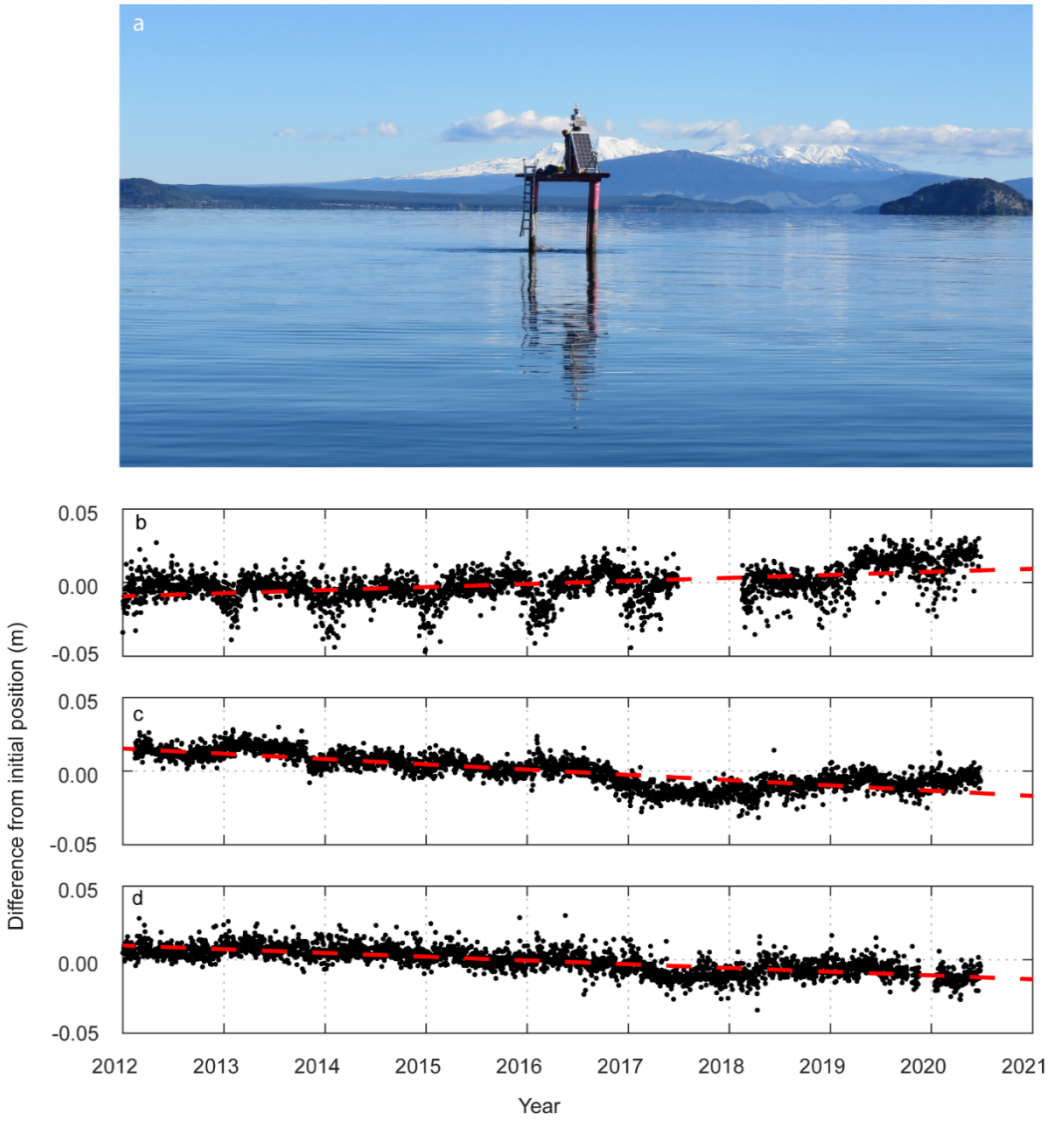

Fig. 3 a Station TGHO on Lake Taupō (looking south to south-west, kindly provided by Brad Scott GNS Science); **b, c and d** Difference from initial ellipsoidal height of station TGHO, 2406 and TGRI between 2012 to 2019 (in ITRF2008)**,** respectively. Their long term linear vertical deformation rates are illustrated as the red-dashed lines

142 TGHO is in a region of active deformation due to regional tectonic, magmatic and local hydrothermal
143 processes (Wallace et al. 2004; Hamling et al. 2015; Holden et al. 2015). Lake levelling surveys
144 conducted between 1979 to 2007, have shown a long-term subsidence trend at the northern part of the
145 lake, punctuated by shorter term localised uplift and subsidence at various locations around the lake
146 (Otway 1989; Otway et al. 2002; Peltier et al. 2009). Fig. 2b indicates that both linear and non-linear
147 vertical motions occur CORS stations around Lake Taupō between 2012 to 2020. Data processing steps
148 for these heights are described at the GeoNet GPS Time Series website (GeoNet, 2020). Heights are
149 provided in the ITRF2008.

150

151 Fig. 3b through Fig. 3d illustrate the change in ellipsoidal heights for station TGHO, 2406 and TGRI in
152 more detail. TGHO shows a strong seasonal signature which is not further investigated here. However,
153 since the GNSS-IR results are in a terrestrial reference frame, the vertical movement of TGHO is
154 accommodated. Stations 2406 and TRGI show a long-term subsidence trend (linear) of 3.7mm/yr and
155 2.8mm/yr, respectively. Similar subsidence rates are assumed to occur at the two nearby lake gauges
156 and to have influenced their lake level observations. These observations were corrected using these
157 linear subsidence rates.

158

159 The GNSS-IR lake surface height retrievals are also compared with satellite radar altimetry lake surface
160 heights. These data are available in the community G-REALM and DAHITI databases. Specific details
161 regarding their processing can be found in Birkett and Beckley (2010), Birkett et al. (2011) and
162 Schwatke et al. (2015). Over the period of this research, 94 lake surface heights were extracted from
163 the DAHITI time-series, based on radar altimetry observations from the Sentinel-3A, Saral and Envisat
164 satellites. From the G-REALM database, 355 estimates were extracted (from radar altimetry
165 observations of the Jason 2 and Jason 3 missions). The approximate ground paths of these satellites are
166 shown in Fig. 2a. All lake surface heights from these were reduced to the WGS-84 ellipsoid. For the G-
167 REALM observations this shift is explained in the data provided from their database. The DAHITI

observations are provided in the EIGEN-6C4 geoid and require conversion to the earth-centered WGS84 datum. An average geoid-ellipsoid value across Lake Taupō (in the EIGEN-6C4 model) was calculated and applied to do this.

GNSS-IR Analysis Details

In GNSS-IR, the user must specify an azimuth mask. At TGHO we excluded observations from satellites between azimuths 135° to 225°. Since low elevation angle data are most impacted by water reflections, only observations from satellites between the angles of 5° to 19° were used. For quality control, we required the amplitude of the LSP peak to be at least 2.7 times greater than the periodogram average over a reflector height region of 2 to 8m. A total of 3382 days of TGHO observations were analysed for this study, yielding ~227,600 individual solutions. The number of lake surface height estimates per day are illustrated in Fig. 4. The median number of individual solutions per day is 69. Only a small minority of days contain less than 20 lake surface height estimates.

Lake Taupō lake surface heights were calculated by subtracting daily H_R estimates from the corresponding daily ellipsoidal heights of station TGHO. However, since ellipsoidal height is defined at the antenna reference point and the GNSS-IR height is measured from the L1 phase centre, an offset exists and must be corrected for. The Zephyr2 geodetic antenna (TRM55971.00 None) at TGHO has a reported L1 phase center offset (UP) of +66.73mm. Therefore, after the H_R estimate was subtracted from the antenna ellipsoid height, a positive correction of 67mm was applied. This is essential to compare the satellite altimetry and GNSS-IR Lake Taupō lake surface heights.

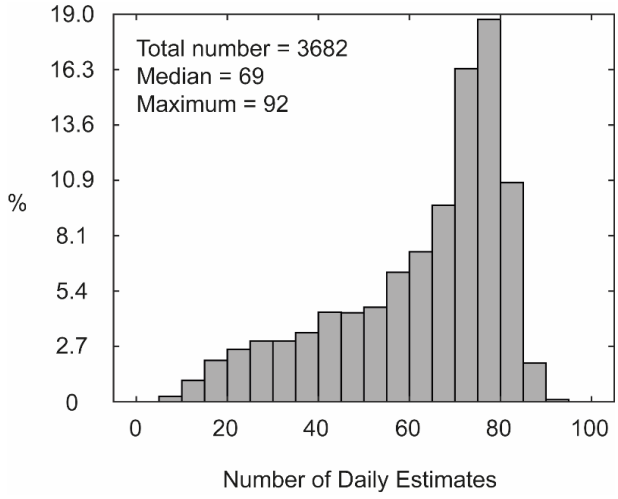

Fig. 4 Solution statistics between 2009 and 2019

For the 2009-2019 period, the Acacia Bay lake gauge dataset is missing ~2% of daily observations. The Tokaanu lake gauge dataset is complete. The data at both instruments is referenced to the Moturiki 1956 Datum (MSL). The lake surface heights derived for TGHO using GNSS-IR are reported in WGS84. As a result, a datum height offset exists between the lake surface heights obtained from the gauges and GNSS-IR.

Results

Gauged lake surface height time series

Fig. 5a shows the daily lake surface height of Lake Taupō at the Tokaanu and Acacia Bay gauges. These are highly correlated (r=0.998) but show fluctuations likely associated with local seasonal patterns of rainfall or snow melt. Their difference (Acacia Bay lake surface height minus Tokaanu lake surface height) (Fig. 5b) show that the lake surface height observed at the gauge at Acacia Bay is lower than that observed at Tokaanu. This difference also increases with time. Fig. 5c shows the same differences

after the trendline in Fig. 5b has been removed. Modelled with a simple linear regression (red line in Fig. 5b), this equates to a yearly difference of -5mm/yr between the two lake gauges. The detrended differences (Fig. 5c) range between ±0.020m to 0.030m, with larger differences present in summer periods. The RMS error of the detrended gauge data in Fig. 5c is ±0.007m**.**

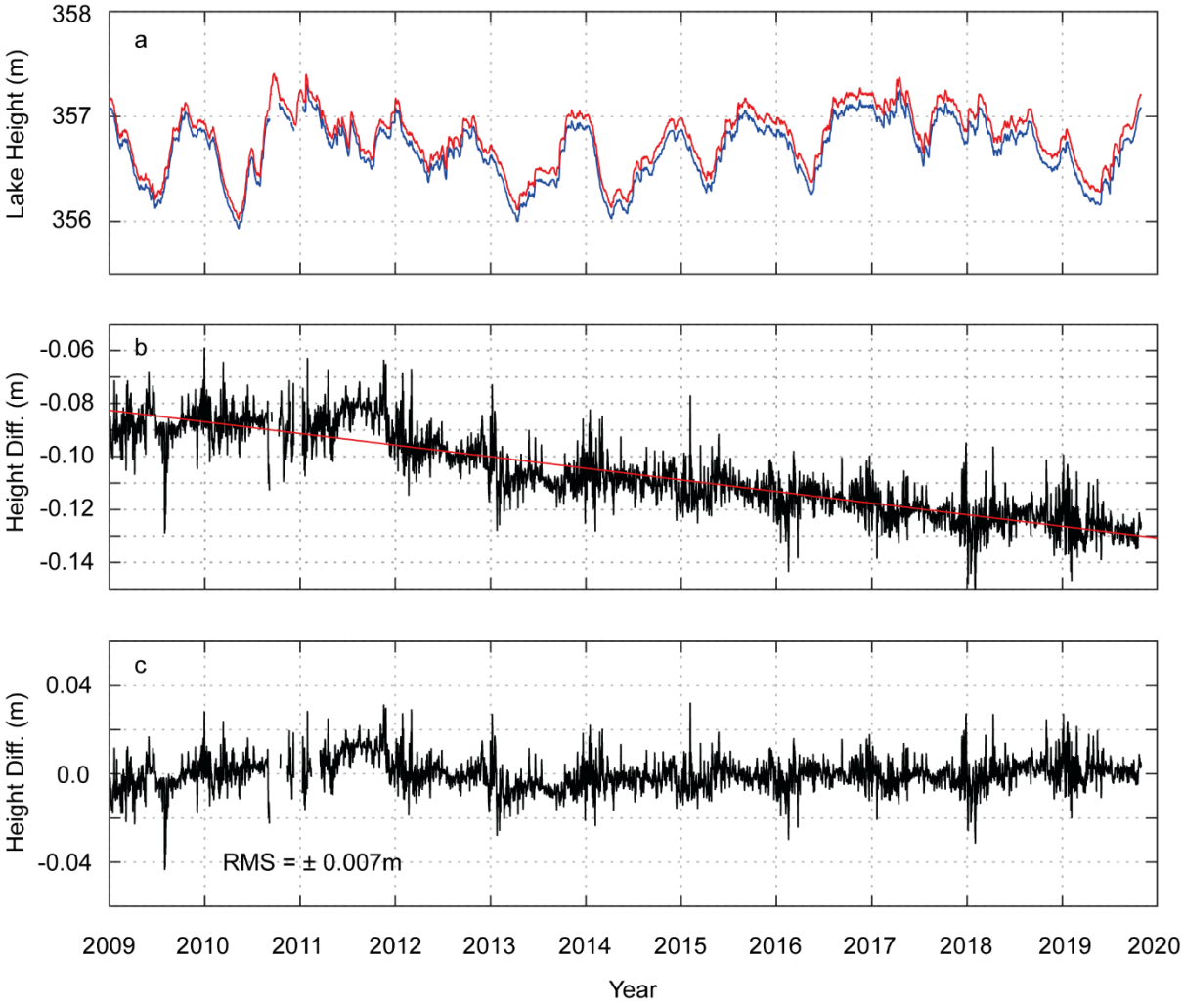

Fig. 5 a The Lake Taupō lake surface height observed at the Tokaanu (red) and Acacia Bay (blue) lake level gauges, respectively. The height (Moturiki Datum) on the y-axis is in metres. **b** the difference (in m) between the lake surface heights observed at the two lake level gauges in Fig. 5a. The red line is the regression fit to these differences; **c** the detrended difference (in m) between the data shown in Fig. 5b

220 *GNSS-IR lake surface height time series*

221

222 The GNSS-IR derived lake surface heights are shown in Fig. 6. These ellipsoidal heights are defined in
223 WGS-84. Outliers were removed in two stages. First, large outliers identified as being greater than 0.5
224 m different from neighbouring estimates were manually removed. Second, remaining outliers were
225 identified using an iterative ten-day moving median average (MAD) filter. In total, the identified
226 outliers reflect approximately 4% of the total estimated surface heights. These were excluded from any
227 further analysis.

228

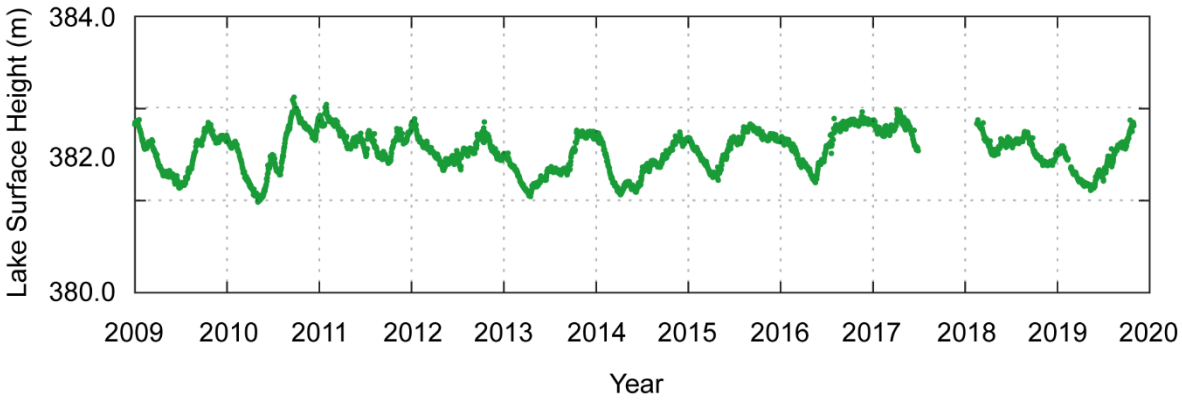

229

230 **Fig. 6** Lake Taupō lake surface height calculated using the GNSS-IR technique at station TGHO. The
231 ellipsoidal height of the lake surface (in m) is shown on the y-axis

232

233 *Comparison of shoreline gauges and GNSS-IR Lake Taupō lake surface heights*

234

235 For purposes of comparison, the lake surface height measurements are converted to relative height
236 differences (relative to their respective first epoch, e.g. 1st Jan 2009). These reflect relative changes in
237 Lake Taupō surface height over time but also accommodate the (unknown) height offset between the
238 Moturiki and the WGS84 datums. Fig. 7a shows the resulting lake surface relative height change

239 observed at Acacia Bay and TGHO; their difference is shown in Fig. 7b. This difference filtered with a
240 five-day moving average filter is shown in Fig. 7c. Fig. 8a to 8c shows the same kind of comparison for
241 the lake gauge at Tokaanu.

242

243 The results show that the lake surface height changes observed from GNSS-IR and lake gauges are
244 highly correlated (0.997 and 0.996 for Acacia Bay and Tokaanu, respectively). The GNSS-IR result
245 captures seasonal changes in the lake surface height that are also evident in the lake gauge observations.
246 Some differences of up to 0.2m occur, but less frequently. The overall RMS difference between the
247 Acacia Bay and GNSS-IR and Tokaanu and GNSS-IR relative lake surface heights are ±0.027m and
248 ±0.028m, respectively. These reduce to ±0.019m and ±0.020m**,** respectively, when the five-day moving
249 average is applied. The distribution of these differences is shown in the histograms in Fig. 9a and 9b.
250 These show a normal distribution, but slightly skewed from zero, particularly in Fig. 9b. The results
251 also show the presence of a time-dependent trend of increasingly larger differences between the GNSS-
252 IR and Tokaanu gauge lake surface heights (Fig. 9b and 9c).

253

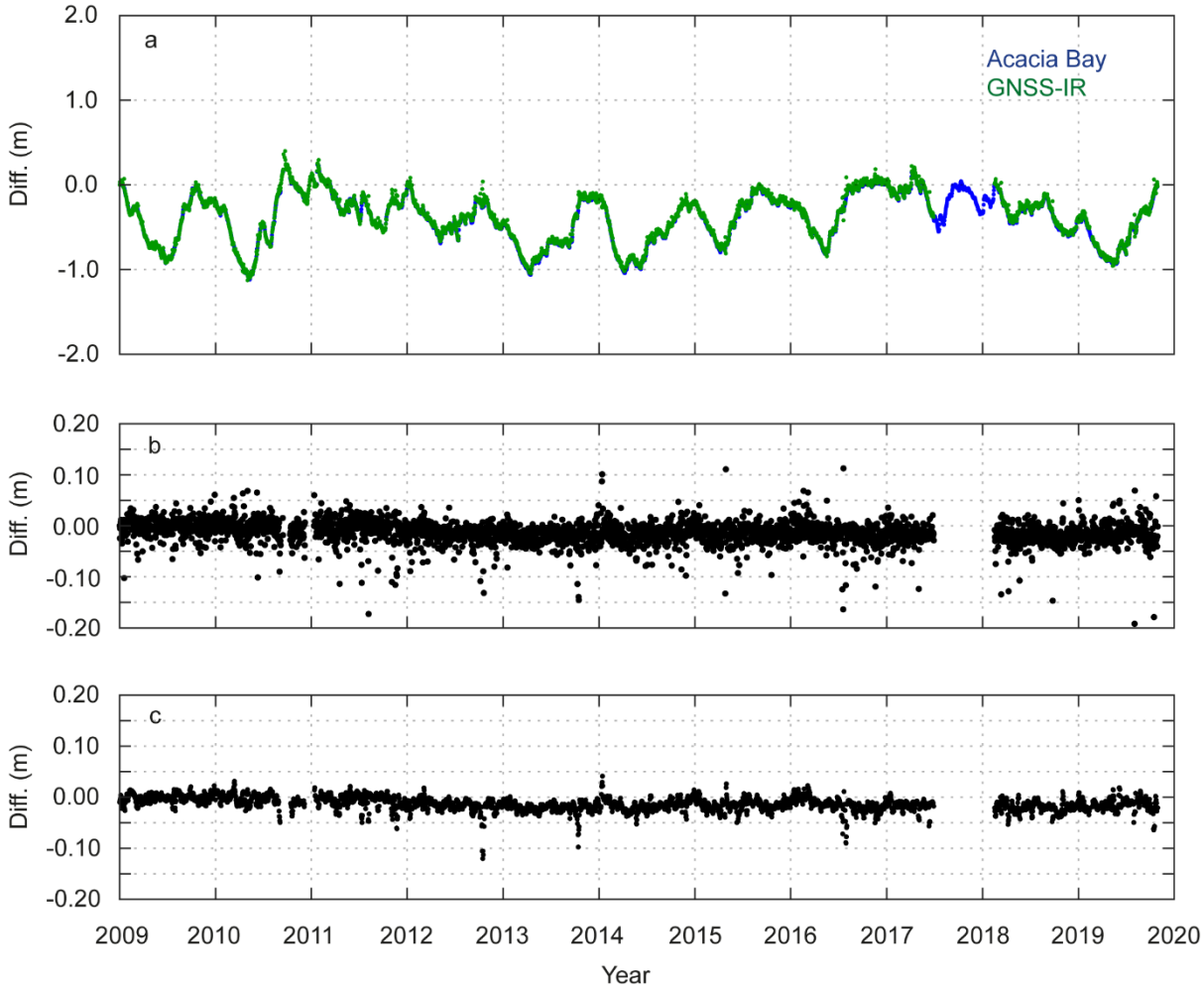

254

255 **Fig. 7 a** Daily lake surface height changes at station TGHO (green) and Acacia Bay gauge (blue) from
256 2009 to 2019; **b** The calculated differences between the two time-series shown in Fig. 7a, RMS
257 ±0.027m; **c** The calculated differences between the two time-series shown in Fig. 7a, of which both
258 have been screened with a five-day moving average filter, RMS ±0.019m

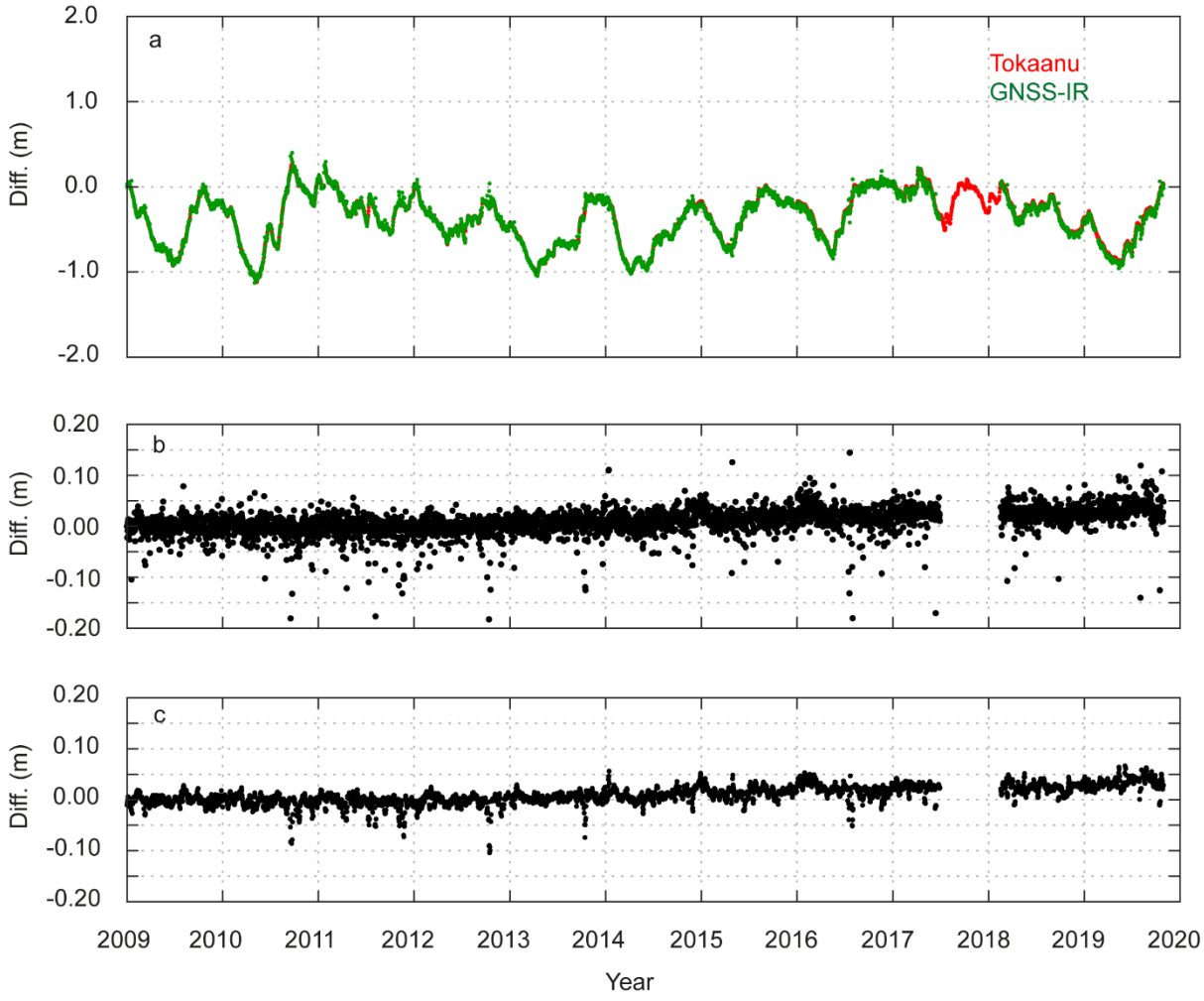

259

260 **Fig. 8 a** Daily lake surface height changes at station TGHO (green) and Tokaanu gauge (red) from 2009
261 to 2019; **b** The calculated differences between the two time-series shown in Fig 8a, RMS ±0.028m; **c**
262 The calculated differences between the two time-series shown in Fig. 8a, of which both have been
263 screened with a five-day moving average filter, RMS ±0.020m

264

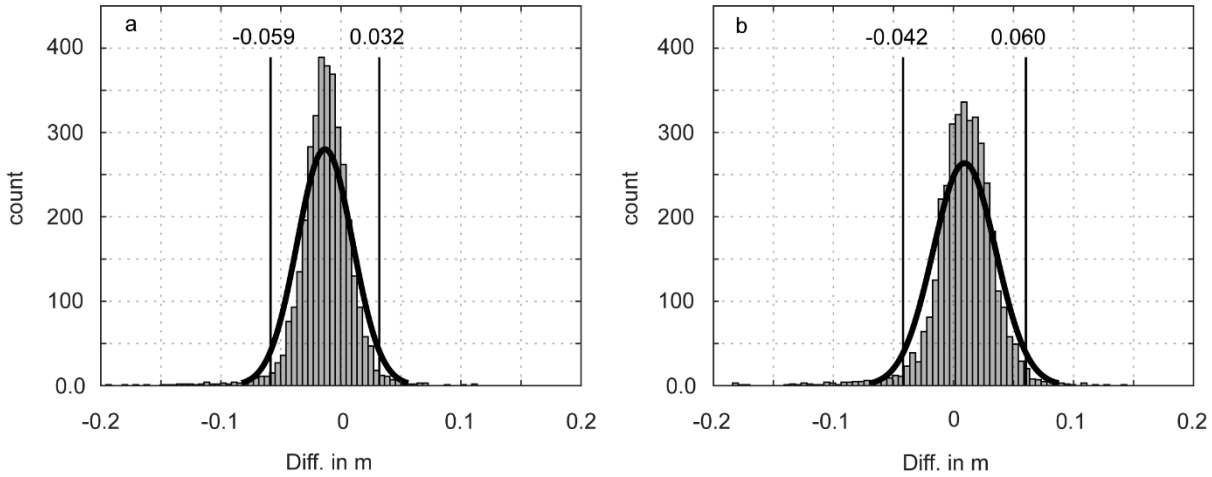

Fig. 9 a Distribution of the differences shown in Fig. 7b; **b** Distribution of the differences shown in Fig. 8b. The upper and lower 95% confidence interval values are annotated (in m) on both figures

Comparison of Satellite altimetry and GNSS-IR time series

The Lake Taupō lake surface height time series from the G-REALM and DAHITI satellite altimetry databases are shown in Fig. 10a. These are plotted alongside the GNSS-IR technique lake surface heights (in WGS-84). The correlation between the two satellite radar altimetry datasets is 0.983. The correlation between the GNSS-IR and satellite radar altimetry lake surface height time series it is 0.921 and 0.940 (for the G-REALM and DAHITI products, respectively). The satellite radar altimetry lake surfaces are higher than the GNSS-IR surface heights (Fig. 10a). This is estimated to be 0.429m between the G-REALM and GNSS-IR lake surface height estimates and 0.210m between the DAHITI and GNSS-IR estimates. To account for this, the satellite altimetric series as treated as relative variations (Fig. 10b). The resulting RMS differences between the GNSS-IR and G-REALM and GNSS-IR and DAHITI lake surface heights are ±0.124m and ±0.069m, respectively.

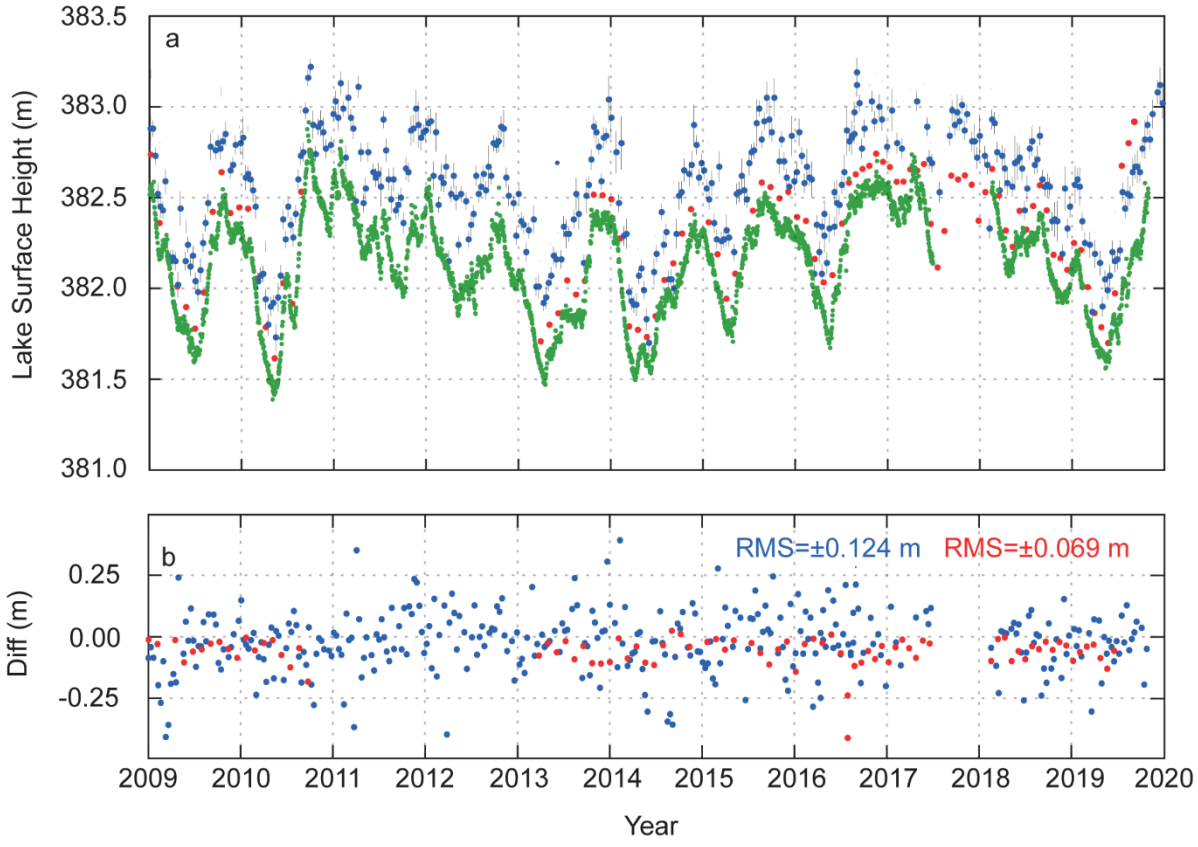

Fig. 10 a Comparison of Lake Taupō lake surface height derived from GNSS-IR technique (green line) and lake surface height derived from G-REALM (blue symbols) and DAHITI (red symbols) data**,** respectively; **b** Relative differences between the time series shown in a. Their respective RMS is shown on the figure

Discussion

The performance of the GNSS-IR technique at TGHO.

Approximately 4% of the daily TGHO solutions were marked as outliers. This indicates that reliable H_R estimates can be obtained at Lake Taupō using GNSS-IR. There is evidence that these daily average H_R outliers are linked to local wind conditions. Fig. 11a plots wind speed at nearby Lake Taupō airport

295 (blue columns) against daily GNSS-IR lake surface heights (black squares) in 2016. The red box
296 highlights a week of increased wind speeds, which is preceded by a week of benign wind conditions.
297 The figure shows that GNSS-IR lake surface height outliers (marked with a red asterisk) are very often
298 correlated with elevated wind speeds (between 6 to 11m/sec). Similar results were identified in the other
299 years of results from this research (not included here).

300

301 Fig. 11b and Fig. 11c show all the periodograms for the reflector height solutions of these two weeks,
302 respectively. The periodograms for the H_R estimates for the week of increased wind speed (Fig. 11b)
303 have decreased power to noise (volts/volts) ratio in comparison to the prior week of decreased wind
304 speeds (Fig. 11c). This is particularly evident over the likely range of reflector heights at station TGHO
305 (e.g. 3 to 4m). An improved GNSS reflection model for estimating sea level and wind speed
306 simultaneously has recently been developed by Reinking et al. (2019) and is an area of future research
307 for us.

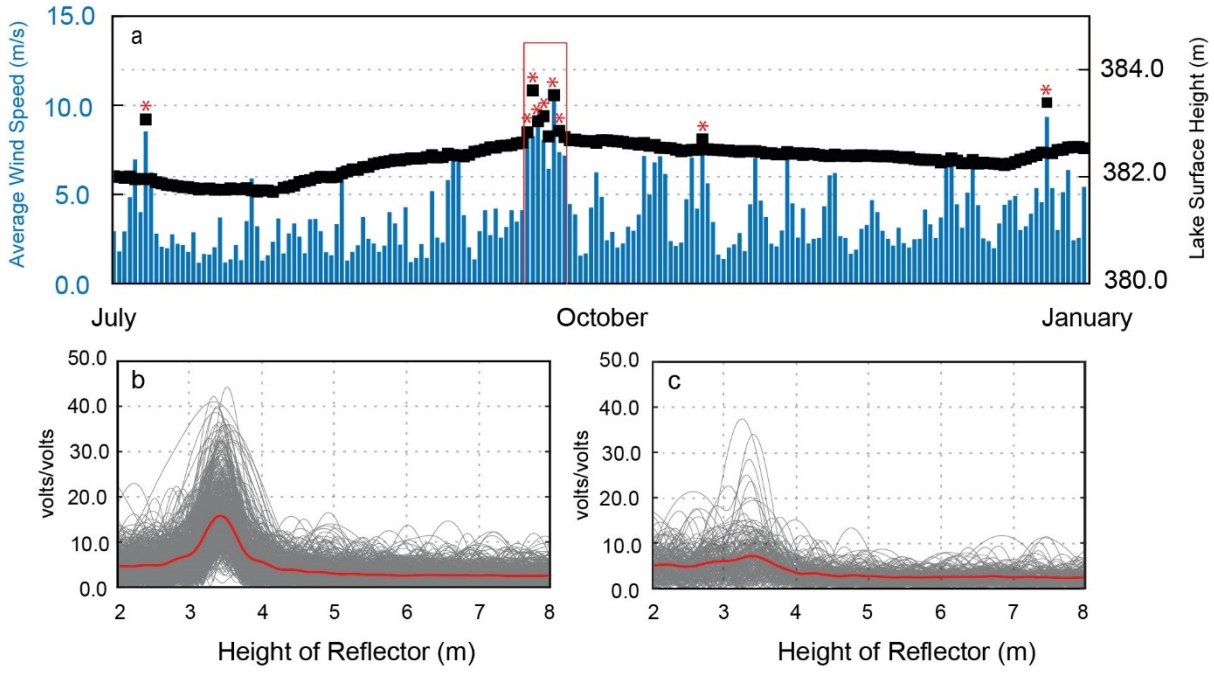

308

309 **Fig. 11 a** Wind speed and lake surface height estimates for 2012. The black solid squares represent the
310 GNSS-IR lake surface heights. The red asterisk shows those heights identified as outliers; **Fig. 11 b** and

311 **c** Periodogram results for the weeks of low and elevated wind speed conditions, respectively. The red
312 lines show the average of all the periodogram solutions over the respective weekly periods

313

314 The lake surface heights measured by GNSS-IR and the gauges are highly correlated (0.997 and 0.996
315 for Acacia Bay and Tokaanu, respectively). Although there are outliers in the daily GNSS-IR lake
316 surface height estimates, they are not frequent enough to obscure both the short and long-term behaviour
317 of the lake over the study period. The relative RMS differences (±0.028m to ±0.027m), calculated
318 between the lake gauge and the GNSS-IR lake surface height time series, agree well with other studies
319 which report RMS differences of a few cm (Larson et al. 2013b, 2017; Lofgren et al. 2014; Song et al.
320 2019). These improve (to ±0.019m to ±0.020m) when a 5-day moving average is applied, however a
321 time-dependent trend is evident. This is particularly evident between Tokaanu lake gauge and TGHO
322 observations after 2012.

323

324 Deformation across the Lake Taupō region is complex (Wallace et al. 2004; Hamling et al. 2015). Lake
325 levelling surveys conducted since 1979, have shown that long-term subsidence has occurred at the
326 northern part of the lake, punctuated by shorter term localised uplift and subsidence at various locations
327 around the lake (Otway 1989; Otway et al. 2002; Peltier et al. 2009). Different rates of uplift and
328 subsidence at TGHO and the two lake gauges complicate the comparison of lake surface heights. The
329 time-dependent trend is likely indicative of un-modelled non-linear deformation associated with
330 regional and/or local magmatic or geothermal processes in the vicinity.

331

332 At present, the vertical deformation rates of the two lake gauge instruments are not monitored
333 continuously in a terrestrial reference frame. Co-located lake gauge and GNSS CORS stations could
334 achieve this and better estimate the deformation at those locations. Connection of the lake gauges to the
335 WGS-84 datum would also allow greater investigation of the QA controls in the GNSS-IR technique at
336 TGHO and absolute comparisons between the satellite altimetry and lake gauge lake surface heights.

337 This highlights the benefit of GNSS-IR at TGHO, as both the vertical movement of the CORS station
338 and the lake surface height of Lake Taupō are observed in WGS84.

339

340 *Comparison with satellite altimetry products*

341

342 The GNSS-IR and satellite radar altimetry lake surface heights (Fig. 10a) (in WGS84) show a high
343 correlation (0.921 and 0.940 for the G-REALM and DAHITI, respectively). However, a bias of 0.429m
344 and 0.210m were identified between the GNSS-IR and the G-REALM and DAHITI lake levels,
345 respectively. When treated as relative differences, a closer agreement was observed between the satellite
346 radar altimetry and GNSS-IR lake surface heights**.** Other studies have identified differences of tens of
347 centimetres to meters between gauge and satellite altimetry observations for small lake bodies,
348 including man made reservoirs (Birkett & Beckley 2010; Ricko et al. 2012; Schwatke et al. 2015).
349 Studies that compare satellite radar altimetry to ground based GNSS field observations of lake levels
350 (not GNSS-IR) found small absolute biases, albeit at larger water bodies. For example, Watson et al.
351 (2011) identified a bias of between +93mm ± 15 mm to +172mm ± 18 mm from ocean buoys in and
352 near Bass Strait in Australia. Cretaux et al. (2018) found bias estimates between +20.6 ± 30 mm to
353 +28.5 ± 20 mm at Lake Issykkul, which is approximately 10 times larger than Lake Taupō.

354

355 The differences observed between the Lake Taupō GNSS-IR and satellite altimetry lake surface heights
356 may be attributed to several error sources in the various satellite altimetry observations across Lake
357 Taupō. Satellite radar altimetry is not a spot height estimate but rather an average within a radar
358 footprint. Local wind affects, lake contours and the different locations of the satellite footprints will
359 pollute the radar waveforms of the different satellite observations differently. The G-REALM surface
360 height time series (which use Jason-2 and 3 observations close to the shoreline – see Fig. 2a) will be
361 different to the DAHITI series. Their proximity to the Lake Taupō shoreline means that terrain effects
362 may contaminate the G-REALM lake level time series. Moreover, the DAHITI product is comprised of

363 the satellite footprint paths at different locations across the lake, observing small differences in the
364 heights of the lake surface. The small size of Lake Taupō (approximately 600km^2) limits its use in
365 current satellite altimetry missions and calibration/validation processes.

366

367 The performance of the ice-retracker algorithm, which is designed to better discern water levels from
368 radar altimetry observations in the presence of ice (Laxon 1995; Gao et al. 2019), may also contribute
369 to the observed differences. In their study, Watson et al. (2011) considered whether the ice-retracker
370 algorithm might have generated shorter satellite altimetry ranges (e.g. higher sea surfaces) compared to
371 their GNSS observed sea surface heights. The results presented here support the presence of a retracker
372 offset between the satellite altimetry datasets. This may be due to the use of different retracking
373 algorithms when processing satellite altimetry radar measurements. Further, the G-REALM and
374 DAHITI products do not contain a correction for the inverse barometer effect. However, Birkett (1995)
375 did not apply a barometric correction since small lake bodies are considered closed systems in
376 comparison to atmospheric systems.

377

378 Some bias may also result from an incorrect slope in the EIGEN-6C4 geoid model (across Lake Taupō)
379 used in the G-REALM and DAHITI products. The spatial resolution of EIGEN-6C4 is similar to the
380 (small) size of Lake Taupō and thus cannot provide great insight. The NZGeoid2016 spatial resolution
381 is approximately 1.8 km (Linz, 2021) and illustrates a N-S slope of approximately 1 to 1.5 meters across
382 Lake Taupō (see Fig. 2a). In the research presented here, we have compared and used products from a
383 community-based satellite altimetry lake database using the global EIGEN-6C4 geoid model. To
384 overcome this limitation, future altimetry measurement reduction at Lake Taupō should incorporate the
385 local NZGeoid2016 model to determine if the geoid slope across Lake Taupō is negligible or whether
386 improved satellite altimetry products are derived.

Implications for Satellite Calibration/Validation techniques and future directions

New missions and novel methods of processing satellite altimetry observations may address some of these limitations. The Surface Water and Ocean Topography (SWOT) mission, to be launched in early 2022, will pass over Lake Taupō with a resolution of a 10 to 70m horizontal resolution (depending on swath angle) with a potential averaged height precision of ±3cm (Neeck et al. 2012). The new CryoSat-2 and Sentinel-3 missions are equiped with a Synthetic Apeture Radar altimeter (SRAL) that generates smaller footprint strips (e.g. 300m and 1km, along and cross-track resolution, respectively) (Santos-Ferreira et al. 2019; Fayad et al. 2020). The novel FF-SAR (Fully focused synthetic aperture radar) technique can be used for SAR altimetry missions such as Cryo-Sat2, Sentinel-3 or Sentinel-6/Jason-CS (Egido 2017). This can reduce along track resolution to half the antenna length and is more suited to smaller lake sizes than traditional radar altimetry (Egido 2017; Kleinherenbrink et al. 2020). Recent testing by Kleinherenbrink et al. (2020) at a medium sized lake identified a 6cm bias between FF-SAR and lake gauge height estimates.

The G-REALM and DAHITI products used here do not incorporate recently available laser altimetry observations from missions such as IceSat2 and Global Ecosystem Dynamics Investigation (GEDI). Due to their smaller footprints (~17m for IceSat2 and ~25m for GEDI) and high-density sampling these are more suitable to small water bodies, and less likely affected by shoreline terrain (Fayad et al. 2020; Yuan et al. 2020). Fayad et al. (2020) found a mean elevation difference of 0.61cm ± 22.3 cm (one standard deviation) between GEDI and in-site lake gauge elevations. Yuan et al. (2020) found that IceSat laser altimetry produced smaller relative altimetric errors and more precise lake surface height than SARAL (radar altimetry) observations following comparisons with lake gauges at over 30 reservoirs in China.

Previous absolute satellite radar altimetry calibration/validation studies (e.g. Watson et al. (2011) and Cretaux et al. (2018)) deployed GNSS receivers at the same time and in the ground track of radar

414 altimetry satellites (e.g. GPS field campaigns). Significant resources are required to undertake these
415 deployments, which makes them difficult and costly to undertake regularly. GNSS-IR presents an
416 opportunity to undertake satellite altimetry cal/val by providing continuous daily lake surface heights
417 in an absolute datum without exhaustive field surveys. In this study, over ten years of daily lake surface
418 heights have been recovered for Lake Taupō using the GNSS-IR technique, with an estimated precision
419 of between 0.020-0.030 m. This is approximately equivalent to the vertical precision achievable using
420 the RTK GPS technique, as utilised by (Cretaux et al. 2018) on Lake Issykkul.

421

422 In this research no single instrument/sensor on any single satellite altimetry mission has been calibrated
423 using the GNSS-IR technique. The merged and highly processed community based DAHITI and G-
424 REALM satellite altimetry products have been used to validate the GNSS-IR lake surface heights and
425 are not suitable for satellite altimetry calibration/validation. Presently, tide gauges are routinely used to
426 calibrate along-track altimeter level-2 product from satellite altimeters. However, our results show that
427 the GNSS-IR technique can provide reliable lake surface heights in a well-defined earth-centered
428 reference frame without conducting costly and exhaustive field work. Concurrently, or after acquisition
429 of satellite radar or laser altimetry observations, the lake surface height could be derived at TGHO by
430 simply downloading the relevant GNSS data and applying the GNSS-IR technique. This provides a
431 cost-effective technique that might be used to calibrate/validate altimetry measurements from new
432 sensors/instruments in future satellite altimetry missions. Continuous and daily lake surface heights at
433 Lake Taupō using GNSS-IR could also be used to assist fine tuning model corrections in these missions.

434

435 ***Conclusions***

436

437 The results presented here show that the GNSS-IR technique provides a reliable long-term estimate of
438 the lake surface height at Lake Taupō in a terrestrial reference frame. The GNSS-IR technique also
439 supplements the existing shoreline gauge instruments at Lake Taupō. A time-dependent trend exists

between the different measurements, but this is almost certainly because of unmodelled ground motion at the two shoreline gauges. It is well appreciated in the satellite altimetry community that systematic error introduced by vertical ground motion at coastal tide gauges must be considered for observations of sea level rise (Mitchum, 2000; Kuo et al. 2004). This work demonstrates similarly that water level measurements on lakes such as Taupō are similarly impacted by regional deformation sources and must be measured. The TGHO GNSS site is unique in that the reflections and positions can be combined to provide water levels in a well defined terrestrial reference frame.

Comparison with satellite radar altimetry lake surface heights identified an absolute bias and may be due to incorrect slope of the EIGEN-6C4 geoid model across Lake Taupō, errors in satellite altimetry measurements and processing or inaccuracies in the lake gauge and GNSS-IR technique. Relative differences between GNSS-IR and satellite radar altimetry lake surface heights were much smaller. Following the launch of new satellite altimetry missions, the GNSS-IR technique at Lake Taupō should be revisited as a calibration/validation site for their altimetry sensors and instruments. It has the potential to become a more cost-efficient technique for satellite altimetry calibration/validation and assist in algorithm development and research. A freely available Lake Taupō lake surface height database could made accessible by all for use as a cross-validation source. To use these kind of GNSS sites for altimetry calibration/validation, they will necessarily need to be located closer to the altimetry tracks. Co-location of a GNSS receiver at the two shoreline gauges at Lake Taupō would significantly improve their contribution to absolute satellite altimetry calibration/validation and better accommodate geologically-driven ground deformation at these locations.

Acknowledgements

The authors are grateful to NIWA and Genesis Energy for permission to access and use the Acacia Bay and Tokaanu lake gauge data; the New Zealand Meteorology Services for access and use of the meteorological data at Taupō AWS; GeoNet and Elisabetta D'Anastasio for access to the GNSS data for TGHO at Lake Taupō.

Author Contributions

LDH conceived the application of the GNSS-IR technique to Lake Taupō and performed the data analysis. LDH and KML wrote and discussed the manuscript.

Data Availability

TGHO and CORS station GNSS RINEX data are freely available via GeoNet ftp from ftp://ftp.geonet.org.nz/gnss. G-REALM satellite altimetry product is available at https://ipad.fas.usda.gov/cropexplorer/global_reservoir/. DAHITI satellite altimetry product is available at https://dahiti.dgfi.tum.de/en/. The Lake Taupō gauge data is available upon request from the National Institute of Water and Atmosphere (NIWA) research (https://niwa.co.nz/). The Taupō Airport meteorological data is available upon request from the New Zealand MetService (https://www.metservice.com/).

Conflict of Interest

The authors declare no conflicts of interest.

488 **References**

489

490 Anderson KD (2000) Determination of water level and tides using interferometric observations of GPS
491 signals, Journal of Atmospheric and Oceanic Technology 17(8):1118-1127.
492 https://doi.org/10.1175/1520-0426(2000)017<1118:DOWLAT>2.0.CO;2

493 Birkett C, (1995) The contribution of TOPEX/POSEIDON to the global monitoring of climatically
494 sensitive lakes. Journal of Geophysical Research 100(C10): 25179-25204

495 Birkett C, Beckley B (2010) Investigating the Performance of the Jason-2/OSTM Radar Altimeter over
496 Lakes and Reservoirs. Marine Geodesy 33:204-238.
497 https://doi.org/10.1080/01490419.2010.488983

498 Birkett C, Reynolds C, Beckley B, Doorn B (2011) From Research to Operations: The USDA Global
499 Reservoir and Lake Monitor. In: Vignudelli S, Kostianoy AG, Cipollini P, Benveniste J (eds) Coastal
500 Altimetry. Springer Berlin Heidelberg, pp. 19-50. https://doi.org/10.1007/978-3-642-12796-0_2

501 Cretaux J, Bergé-Nguyen M, Calmant S, Jamangulova N, Satylkanov R, Lyard F, Perosanz F, Verron
502 J, Samine Montazem A, Guilcher G, Leroux D, Barrie J, Maisongrande P, Bonnefond P (2018)
503 Absolute Calibration or Validation of the Altimeters on the Sentinel-3A and the Jason-3 over Lake
504 Issykkul (Kyrgyzstan). Remote Sensing 10(11). https://doi.org/10.3390/rs10111679

505 Dunne S, Soulat F, Caparrini M, Germain O, Farrés E, Barroso X, Ruffini, G (2005) Oceanpal® a GPS-
506 reflection coastal instrument to monitor tide and sea-state. In: Proceedings of the International
507 Geoscience and Remote Sensing Symposium (IGARSS). Barcelona, Spain, July 23-28, 2007

508 Egido A, (2017) Fully Focussed SAR Altimetry: Theory and Applications. IEEE Transactions of
509 Geoscience and Remote Sensing 55(1). Doi 10.1109/TGRS.2016.2607122

510 Eser P, Rosen M, 2000 Effects of artificially controlling levels of Lake Taupō, North Island, New
511 Zealand, on the Stump Bay wetland, New Zealand Journal of Marine and Freshwater Research,
512 34(2):217-230, DOI: 10.1080/00288330.2000.9516928

513 Fayad I, Baghdadi N, Bailly JS, Frappart F, Zribi M, (2020) Analysis of GEDI elevation data accuracy
514 for inland waterbodies altimetry. Remote Sensing 12(17):2714. https://doi.org/10.3390/rs12172714

515 Gao Q, Makhoul E, Escorihuela MJ, Zribi M, Quintana Seguí P, García P, Roca M (2019) Analysis of
516 Retrackers' Performances and Water Level Retrieval over the Ebro River Basin Using Sentinel-3.
517 Remote Sensing. 11(6):718. https://doi.org/10.3390/rs11060718

518 GeoNet (2020) GNSS Time Series Notes. Geological and Nuclear Sciences New Zealand.
519 https://www.geonet.org.nz/data/ supplementary/gnss_time_series_notes. Accessed on 14/07/2020

520 Hamling IJ, Hreinsdóttir S, Fournier N (2015) The ups and downs of the TVZ: Geodetic observations
521 of deformation around the Taupō Volcanic Zone, New Zealand. Journal of Geophysical Research
522 Solid Earth 120(6): 4667-4679. https://doi.org/10.1002/2015JB012125

523 Holden L, Wallace L, Beavan J, Fournier N, Cas R, Ailleres L, Silcock D (2015) Contemporary ground
524 deformation in the Taupō Rift and Okataina Volcanic Centre from 1998 to 2011, measured using
525 GPS. Geophysical Journal International 202(3): 2082-2105. https://doi.org/10.1093/gji/ggv243

526 Kleinherenbrink K, Naeije M, Slobbe C, Egido A, Smith W (2020) The performance of CryoSat-2 fully
527 focussed SAR for inland water level. Remote Sensing of the Environment 237(111589)
528 https://doi.org/10.1016/j.rse.2019.111589

529 Kuo CY, Shum CK, Braun A, Mitrovica JX (2004) Vertical crustal motion determined by satellite
530 altimetry and tide gauge data in Fennoscandia. Geophysical Research Letters 31(1).
531 doi:10.1029/2003GL019106.

532 Larson KM, Lofgren JS, Haas R (2013a) Coastal sea level measurements using a single geodetic GPS
533 receiver. Advances in Space Research 51(8):1301-1310. DOI: 10.1016/j.asr.2012.04.017

534 Larson, KM, Ray, RD, Nievinski, FG & Freymueller, JT (2013b), The Accidental Tide Gauge: A GPS
535 Reflection Case Study From Kachemak Bay, Alaska, Ieee Geoscience and Remote Sensing Letters,
536 (10) 5:1200-1204.

Larson KM, Nievinski FG (2013) GPS snow sensing: results from the EarthScope Plate Boundary Observatory. GPS Solutions 17(1):41-52. DOI: 10.1007/s10291-012-0259-7

Larson KM, Ray RD, Williams SDP (2017) A 10-Year Comparison of Water Levels Measured with a Geodetic GPS Receiver versus a Conventional Tide Gauge. Journal of Atmospheric and Oceanic Technology 34(2): 295-307. https://doi.org/10.1175/JTECH-D-16-0101.1

Laxon S (1994) Sea ice altimeter processing scheme at EODC. International Journal of Remote Sensing 15(4): 915-924. DOI: 10.1080/01431169408954124

LINZ (2021) New Zealand Quasigeoid 2016 (NZGeoid2016). Land Information New Zealand. https://www.linz.govt.nz/data/geodetic-system/datums-projections-and-heights/vertical-datums/new-zealand-quasigeoid-2016-nzgeoid2016. Accessed on 11/04/2021

Löfgren J, Haas R, Johansson J (2009) Sea Level Monitoring Using a GNSS-Based Tide Gauge. In: Proceedings of the 2nd International Colloquium - Scientific and Fundamental Aspects of the Galileo Programme. Padua, Italy, 14-16 October, 2009.

Martin-Neira M (1993) A Passive Reflectometry and Interferometry System (PARIS): Application to ocean altimetry. ESA Journal, 17:331-355.

Mitchum G (2000) An Improved Calibration of Satelilte Altimetric Heights Using Tide Gauge Sea Levels with Adustment for Land Motion. Marine Geodesy 23(3). https://doi.org/10.1080/01490410050128591

Neeck S, Lindstrom E, Vaze P, Fu, L-L (2012) Surface Water and Ocean Topography (SWOT) mission. In Proceedings of SPIE 8533, Sensors, Systems, and Next-Generation Satellites XVI. Edinburgh, United Kingdom, 19 November, 2012. https://doi.org/10.1117/12.981151

Otway P, Blick G, Scott B (2002) Vertical deformation at Lake Taupō, New Zealand, from lake levelling surveys, 1979–99. New Zealand Journal of Geology and Geophysics, 45:121-132. https://doi.org/10.1080/00288306.2002.9514964

561 Otway PM (1989) Vertical Deformation Monitoring by Periodic Water Level Observations, Lake
562 Taupō, New Zealand. In: Latter J (ed) Volcanic Hazards. Springer, Berlin Heidelberg, pp. 561-574.

563 Peltier A, Hurst T, Scott B, Cayol V (2009) Structures involved in the vertical deformation at Lake
564 Taupō (New Zealand) between 1979 and 2007: New insights from numerical modelling. Journal of
565 Volcanology and Geothermal Research, 181(3):173-184.
566 https://doi.org/10.1016/j.jvolgeores.2009.01.017

567 Reinking J, Roggenbuck O, Even-Tzur G (2019) Estimating Wave Direction Using Terrestrial GNSS
568 Reflectometry. Remote Sensing 11(19):11. DOI: 10.3390/rs11091027

569 Ricko M, Birkett C, Carton J, Cretaux J (2012) Intercomparison and validation of continental water
570 level products derived from satellite radar altimetry. Journal of Applied Remote Sensing 6:1710.
571 DOI: 10.1117/1.JRS.6.061710

572 Roesler C, Larson KM (2018) Software tools for GNSS interferometric reflectometry (GNSS-IR). GPS
573 Solutions 22(3). https://doi.org/10.1007/s10291-018-0744-8

574 Roggenbuck O, Reinking J (2019) Sea Surface Heights Retrieval from Ship-Based Measurements
575 Assisted by GNSS Signal Reflections. Marine Geodesy 42(1):1-24.
576 https://doi.org/10.1080/01490419.2018.1543220

577 Roussel N, Ramillien G, Frappart F, Darrozes J, Gay A, Biancale R, Striebig N, Hanquiez V, Bertin X,
578 Allain D (2015) Sea level monitoring and sea state estimate using a single geodetic receiver. Remote
579 Sensing of Environment 171:261-277. https://doi.org/10.1016/j.rse.2015.10.011

580 Santamaria-Gomez A, Watson C, Gravelle M, King M, Woppelmann G (2015) Levelling co-located
581 GNSS and tide gauge stations using GNSS reflectometry. Journal of Geodesy 89(3):241-258. DOI:
582 10.1007/s00190-014-0784-y

583 Santos-Ferreira A, da Silva J, Magalhaes J, (2018) SAR Mode Altimetry Observations of Internal
584 Solitary Waves in the Tropical Ocean Part 1: Case Studies. Remote Sensing 10(4):644.
585 https://doi.org/10.3390/rs10040644

586 Schwatke C, Dettmering D, Bosch W, Seitz F (2015) DAHITI – an innovative approach for estimating
587 water level time series over inland waters using multi-mission satellite altimetry. Hydrology and
588 Earth Science Systems 19(10) 4345-4364. https://doi.org/10.5194/hess-19-4345-2015

589 Song MF, He XF, Wang XL, Zhou Y, Xu, XY (2019) Study on the Quality Control for Periodogram in
590 the Determination of Water Level Using the GNSS-IR Technique. Sensors 19(20). doi:
591 10.3390/s19204524

592 Strandberg J, Hobiger T, Haas R, (2016) Improving GNSS-R sea level determination through inverse
593 modeling of SNR data. Radio Science 51(8):1286-1296. https://doi.org/10.1002/2016RS006057

594 Sun J (2017) Ground-Based GNSS-Reflectometry Sea Level and Lake Ice Thickness Measurements.
595 PhD thesis dissertation, The Ohio State University, US.

596 Treuhaft RN, Lowe ST, Zuffada C, Chao Y (2001) 2-cm GPS altimetry over Crater Lake. Geophysical
597 Research Letters 28(23): 4343-4346. https://doi.org/10.1029/2001GL013815

598 Wallace LM, Beavan J, McCaffrey R, Darby D (2004) Subduction zone coupling and tectonic rotations
599 in the North Island, New Zealand. Journal of Geophysical Research 109:B12406.
600 https://doi.org/10.1029/2004JB003241

601 Watson C, White N, Church J, Burgette R, Tregoning P, Coleman R (2011) Absolute calibration in
602 Bass Strait, Australia: TOPEX, Jason-1 and OSTM/Jason-2. Marine Geodesy 34:242-260.
603 https://doi.org/10.1080/01490419.2011.584834

604 Williams SDP, Nievinski FG (2017) Tropospheric delays in ground-based GNSS multipath
605 reflectometry-Experimental evidence from coastal sites. Journal of Geophysical Research-Solid
606 Earth 122(3)2310-2327. https://doi.org/10.1002/2016JB013612

607 Yuan C, Gong P, Bai Y, (2020) Performance assessment of ICESat-2 laser altimeter data for water-
608 level measurement over lakes and reservoirs in China. Remote Sensing 12(5):770.
609 https://doi.org/10.3390/rs12050770